





ARTICLE

Outer retinal and choriocapillaris modifications in choroideremia: three differentially impaired retinal regions and the potential diagnostic role of the external limiting membrane

Alessandro Arrigo¹ , Maurizio Battaglia Parodi¹, Emanuela Aragona¹, Adelaide Pina¹, Francesca Calcagno¹, Francesco Bandello¹ and Robert E. MacLaren^{1,2} 

© The Author(s), under exclusive licence to The Royal College of Ophthalmologists 2022

BACKGROUND: The external limiting membrane (ELM) is formed by the apical processes of Müller cells attached to the inner segments of the photoreceptor cells. Both cells are implicated in the pathogenesis of choroideremia (CHM). The purpose of this study was to explore the diagnostic role of ELM in CHM.

METHODS: The study was designed as observational case series. Sixteen CHM eyes were examined by multimodal imaging and were compared to healthy controls. The main outcome was the measurement of ELM thickness and reflectivity over the follow-up, and its relationship with other multimodal imaging quantitative parameters.

RESULTS: Baseline ELM was characterized by $11 \pm 1 \mu\text{m}$ of thickness and 0.68 ± 0.13 of reflectivity, resulting $8 \pm 1 \mu\text{m}$ ($p < 0.01$) and 0.65 ± 0.14 ($p > 0.05$) at the last follow-up. Choriocapillaris (CC) analysis revealed 3 regions. The first was characterized by normal vessel density (VD). The second surrounding the partially preserved islet, showing significantly lower baseline VD and undergoing minor changes over the follow-up. The third was localized in the partially preserved islet, showing significantly lower VD at baseline, and resulted atrophic at the last follow-up. ELM reflectivity and ELM thickness correlated both with outer retinal atrophy progression and the CC status.

CONCLUSIONS: ELM may be considered a useful imaging biomarker in CHM. Its assessment confirmed a primary role of Müller cells impairment in the pathogenesis of CHM.

Eye (2023) 37:338–343; <https://doi.org/10.1038/s41433-022-01953-3>

INTRODUCTION

Choroideremia (CHM) is a genetically determined retinal dystrophy. It is characterized by a progressive and visually impairing centripetal chorioretinal degeneration [1–4]. The X-linked genetic defect was identified in the *CHM* gene encoding Rab Escort protein-1, a protein mainly localized in the retinal pigment epithelium (RPE) and regulating the intracellular vesicle trafficking [5]. Although degeneration of the outer retina and the RPE represents the most evident clinical finding, an intriguing hypothesis suggested Müller cells might also provide a primary site of pathogenesis [6]. These specialized glial cells govern several metabolic functions within the retina and are located between the internal limiting membrane (ILM) and the external limiting membrane (ELM), which are extensions of the Müller cell structure [7]. Whereas the ILM is poorly visualized and isolated from the other structures on structural optical coherence tomography (OCT), ELM is easily detectable and measurable, corresponding to the hyperreflective structure under the hyporeflexive outer nuclear layer. ELM may represent a useful biomarker to monitor the evolution of CHM, but there are no reliable data concerning its modification over the follow-up.

The main goal of the present study is to quantitatively investigate change in ELM thickness and reflectivity from baseline to last follow-up visit in CHM and to analyze the relationship with the clinical features of the disease and its progression.

MATERIALS AND METHODS

The study was designed as prospective, observational, case series. Patients affected by CHM, confirmed by the genetic assessment of *CHM* gene mutation, were recruited from the Inherited Retinal Dystrophy Unit of the Scientific Institute San Raffaele Hospital, and followed up for at least 2 years. All the patients provided a written informed consent. The study adhered to the Declaration of Helsinki and was approved by the Ethical Committee of Scientific Institute San Raffaele Hospital (MIRD). Exclusion criteria were cystoid macular oedema, refractive errors greater than $\pm 3\text{D}$, ophthalmic surgeries in the last six months from the inclusion, systemic conditions potentially affecting our analyses. For the quantitative comparisons, we included also a cohort of healthy age- and refractive-matched male subjects. The ophthalmologic investigation included best-corrected visual acuity (BCVA), slit-lamp anterior and posterior biomicroscopy, Goldmann applanation tonometry, blue-light fundus autofluorescence (BL-FAF), structural OCT (Spectralis HRA2 + OCT, Heidelberg Engineering;

¹Department of Ophthalmology, IRCCS San Raffaele Scientific Institute, via Olgettina, 60, 20132 Milan, Italy. ²Oxford Eye Hospital, Oxford University Hospitals NHS Foundation Trust, and Nuffield Laboratory of Ophthalmology, Nuffield Department of Clinical Neurosciences, University of Oxford, Oxford, UK. ✉email: alessandro.arrigo@hotmail.com

Received: 20 September 2021 Revised: 6 January 2022 Accepted: 19 January 2022

Published online: 28 January 2022

Table 1. Quantitative OCT and OCTA analysis of 16 choroideremia eyes and 20 age-matched controls.

Quantitative OCT and OCTA analysis				
	Baseline	Last F/U	Controls	p Value
CMT (μm)	242 ± 18	238 ± 21	241 ± 11	>0.05
Mean ELM Thickness (μm)	11 ± 1	8 ± 1	13 ± 1	<0.01
ELM Thickness in the region of atrophy progression (μm)	8 ± 1	0 ± 0	N/A	N/A
Mean ELM Reflectivity	0.68 ± 0.13	0.65 ± 0.14	0.68 ± 0.06	>0.05
ELM Reflectivity in the region of atrophy progression	0.49 ± 0.25	N/A	N/A	N/A
Partially preserved islet area (mm^2)	10 ± 7	7 ± 5	N/A	N/A
Partially preserved islet area + Surrounding Borders (mm^2)	12 ± 5	9 ± 4	N/A	N/A
VD SCP	0.4 ± 0.02	0.39 ± 0.03	0.4 ± 0.02	>0.05
VD DCP	0.02 ± 0.01	0.02 ± 0.02	0.4 ± 0.03	<0.01
VD CC Mean	0.5 ± 0.02	0.49 ± 0.03	0.5 ± 0.02	>0.05
VD CC Partially Preserved Islet	0.5 ± 0.04	0.49 ± 0.03	0.5 ± 0.02	>0.05
VD CC Surrounding Borders	0.41 ± 0.05	0.39 ± 0.02	0.5 ± 0.02	<0.01
VD CC in the region of atrophy progression	0.42 ± 0.08	0.39 ± 0.05	0.5 ± 0.02	<0.01

CMT central macular thickness, ELM external limiting membrane, VD vessel density, SCP superficial capillary plexus, DCP deep capillary plexus, CC choriocapillaris.

Heidelberg, Germany) and OCT angiography (OCTA) (DRI Triton OCT, Topcon Corporation, Tokyo, Japan). Structural OCT acquisitions included enhanced depth imaging (EDI) radial, raster and dense scans (ART > 25). OCTA data were obtained from 4.5×4.5 mm and 12×12 mm acquisitions.

The main outcome of the study was the measurement of thickness and reflectivity of ELM over the follow-up. Secondary outcomes included the relationship with atrophy progression as assessed on enface OCT and BL-FAF.

Central macular thickness (CMT) was automatically extracted from the Heidelberg software data. ELM thickness measure was obtained on a horizontal, foveal scan. In order to achieve a reliable standardization of the measurements, with respect to the different aspects of the partially preserved retinal islet characterizing CHM eyes, we performed the following steps. First of all, we obtained a linear measure of the extension of the partially preserved islet on the structural OCT scan. Then, we subdivided this section in five equally distanced points, in order to

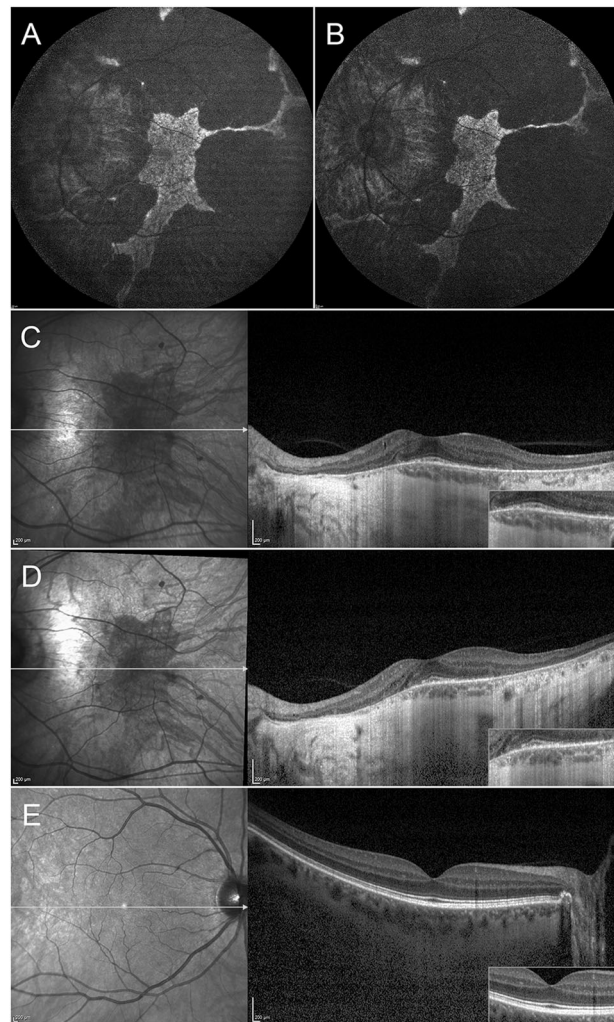


Fig. 1 The relationship between ELM status and atrophy progression. BAF images disclose evident shrinkage of the partially preserved retinal islet over the follow-up (A, B). The baseline structural OCT evaluation visually shows that the retinal region undergoing atrophy progression is characterized by a thinner and less reflective ELM, with respect to the central portion of the partially preserved retinal islet (C, D). Structural OCT of healthy control is provided in (E) for comparison.

calculate the ELM thickness. The mean value was included in the statistical analysis. For the healthy controls, we considered the following points: subfoveal, $750 \mu\text{m}$ (right-left) and $1500 \mu\text{m}$ (right-left). Also in this case, the mean value was considered as the final ELM thickness (Supplementary Fig. 1). The measurement tool provided in Heidelberg software was employed for the analyses.

ELM reflectivity was obtained from the same structural OCT scans, exporting the images in.tiff format. Then, the images were loaded in Fiji software (<https://imagej.net/Fiji/Downloads>). An expert grader (AA) manually segmented the ELM only in the region considered for the thickness measure, and the Fiji tool Analyze->Measure was used to extract the mean ELM reflectivity value. A second analysis regarded the reflectivity measure only of the ELM localized in the region undergoing atrophy progression. Additional investigations regarded the relationship between ELM features and the development of outer retinal tubulations (ORT).

OCTA 12×12 mm reconstructions were used to extract vessel density (VD) values for the superficial (SCP), deep capillary (DCP) and choriocapillaris (CC) plexuses, respectively. Two expert graders (AA and EA) evaluated the automatic segmentations of the plexuses, which were eventually manually modified. All the reconstructions were loaded in Fiji software (<https://imagej.net/Fiji/Downloads>) and were binarized through

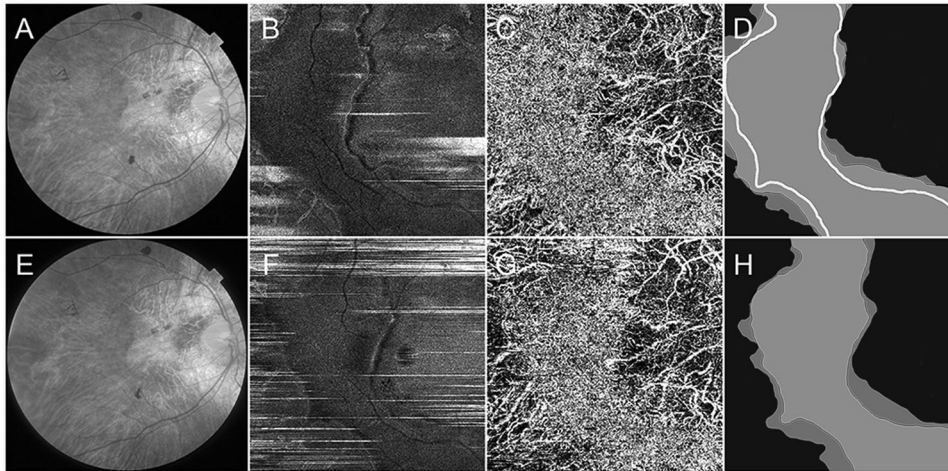


Fig. 2 The detection of the three different CC regions in CHM. Baseline colour fundus, enface OCT and OCTA status are shown in **A**, **B** and **C**, respectively. Enface OCT well detected the borders of the partially preserved retinal islet. The overlap between the partially preserved retinal islet area (blue) and the CC area (red) allows to identify the CC area extending over the surrounding borders. Furthermore, the adding of the partially preserved islet detected on enface OCT at the last follow-up (yellow line) allows to isolate the CC region undergoing atrophic changes (**D**). Last follow-up images show the evident reduction of the considered regions (**E**, **F**, **G**, respectively). Interestingly, the mismatch between the partially preserved retinal islet area (blue) and the CC area (red) is still present at the end of the follow-up (**H**) (colour figure online).

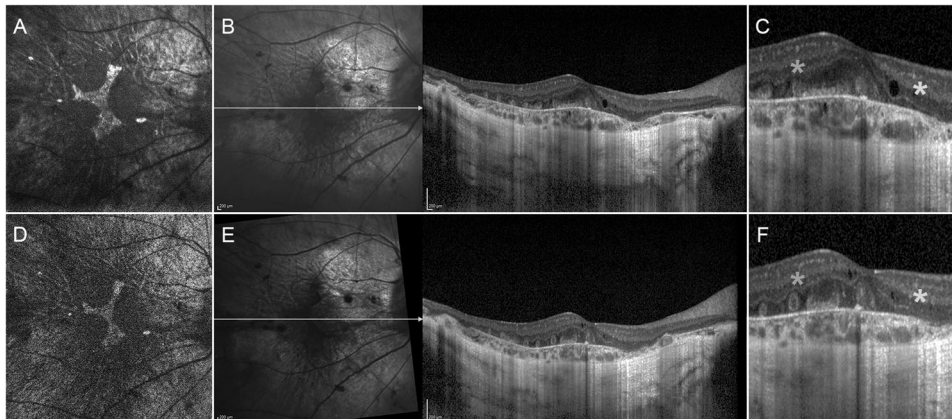


Fig. 3 ORT formation in CHM. The figure discloses baseline BAF, structural OCT and magnified structural OCT (**A**, **B**, **C**, respectively) and last follow-up images (**D**, **E**, **F**, respectively). Although some ORT are already present at baseline, during the follow-up it is possible to see the further development of a ORT at the border of the partially preserved retinal islet area. The mandatory condition for the ORT formation is the presence of a partially preserved ellipsoid zone at baseline (orange asterisk). In the absence of this condition, it is possible to observe only some minor atrophic changes (blue asterisk), making the progression of outer retinal atrophy somehow symmetric. The ORT formation is followed also by the progression of outer retinal atrophy, as evinced by the expansion of the window “bar code” effect detected by structural OCT (colour figure online).

a “mean” automatic threshold. Foveal avascular zone was manually segmented and excluded. Then, VD was calculated as the ratio between white and black pixels [8]. We considered only the VD values of the partially preserved islet.

Atrophy progression was assessed both on BAF and on enface 12×12 mm OCT images by the same two expert graders, using the segmentation tool provided by ImageNET6 Topcon software. Furthermore, we measured the total area of CC extension, detected on OCTA. We evaluated the difference between the areas measured on enface 12×12 mm OCT and on OCTA images, thus separately considering the area of the partially preserved retinal islet and the area covered by the surrounding borders. Then, we performed a separated VD measure of these two CC areas. Furthermore, we performed a quantification of the CC VD in the borders of the partially preserved islet region over the follow-up. To sum up the subdivision of CC VD analysis, we separately considered: (1) partially preserved islet; (2) region of the partially preserved islet evolving to atrophy over the last follow-up; (3) CC region surrounding the borders of the partially preserved islet. All the quantitative measures were taken at least twice by two experts (AA, EA) to test reproducibility and repeatability. Interclass correlation coefficient (ICC) was also calculated to test the agreement between the two readers.

For the statistical analysis, we considered only the baseline and the last follow-up measurements. Continuous variables were analyzed through two-tailed *T* test. The correlations among the collected parameters were explored using Tau-b Kendall correlation test. Statistical significance was set to $p < 0.05$. All the analyses were performed using SPSS Statistics Version 21.0 Software package (IBM; Armonk, NY).

RESULTS

We included 16 eyes of 8 patients (mean age 39 ± 14 years) and 20 eyes of 20 healthy male controls (mean age 40 ± 10 years) ($p > 0.05$). The mean follow-up was of 3.5 ± 1.4 years. Mean LogMAR BCVA was 0.0 ± 0.0 for both groups ($p > 0.05$).

All the findings of the quantitative analysis are reported in Table 1.

Mean baseline ELM thickness was 11 ± 1 μm , reducing to 8 ± 1 μm ($p < 0.01$) at the end of the follow-up. Mean ELM reflectivity was 0.68 ± 0.13 at baseline, changing to 0.65 ± 0.14 ($p > 0.05$) at the end of the follow-up. Although ELM thickness resulted lower than

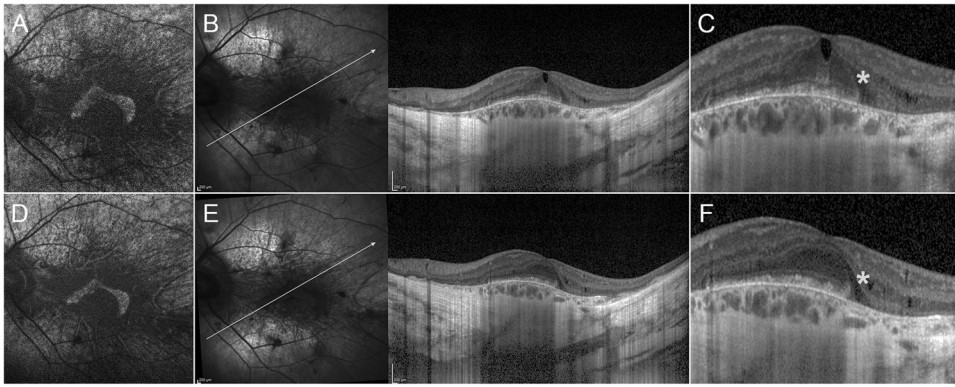


Fig. 4 Atrophy progression in CHM without the onset of ORT. The figure discloses baseline BAF, structural OCT and magnified structural OCT (A, B, C, respectively) and last follow-up images (D, E, F, respectively). Differently from Fig. 4, in this case it is possible to observe an asymmetric progression of the outer retinal atrophy. Indeed, in the presence of a partially preserved ellipsoid zone at baseline (blue asterisk), we detected an evident reduction of the partially preserved retinal islet, with extension of the window “bar code” effect, only in the left part of the structural OCT image, whereas the right side discloses almost stable conditions over the follow-up (colour figure online).

healthy controls ($13 \pm 1 \mu\text{m}$) both at baseline and at the end of the follow-up ($p < 0.01$), ELM reflectivity was not statistically different compared to controls (0.68 ± 0.13) ($p > 0.05$). Interestingly, ELM thickness ($8 \pm 1 \mu\text{m}$) and ELM reflectivity (0.49 ± 0.25) of the borders evolving towards atrophy resulted significantly worse with respect to both partially preserved islet and healthy controls ($p < 0.01$). The modifications of the ELM and of the outer retina are shown in Fig. 1.

With respect to VD analysis, DCP resulted significantly altered ($p < 0.01$) (Table 1). The analysis of CC revealed three different regions. In particular, the first CC region corresponded to the partially preserved islet, with CC VD resulted preserved, compared to healthy controls (0.5 ± 0.04 vs 0.5 ± 0.02 ; $p > 0.05$).

The second region corresponded to CC region surrounding and extending beyond the borders of the partially preserved islet (Supplementary Fig. 2), which disclosed a significantly reduced VD at baseline (0.41 ± 0.05 ; $p < 0.01$) and underwent minor changes at the last follow-up (0.39 ± 0.02 ; $p > 0.05$). Interestingly, the CC area covered by the partially preserved islet associated with the CC surrounding borders resulted larger than the partially preserved islet area alone, although not reaching the statistical significance (12 ± 5 vs $10 \pm 7 \text{ mm}^2$; $p > 0.05$), with no significant area reductions at the end of the follow-up (9 ± 4 and $7 \pm 5 \text{ mm}^2$; $p > 0.05$).

The third CC region was represented by the region of the partially preserved islet undergoing atrophic changes at the last follow-up (Fig. 2). This region disclosed a significantly reduced CC VD at baseline, compared to the rest of the partially preserved islet (0.42 ± 0.08 vs 0.5 ± 0.04 ; $p < 0.01$) and did not show significant changes over the follow-up (0.39 ± 0.05) ($p > 0.05$). It is worth of notice the correspondence of the VD values between the CC in the region of atrophy progression and the CC of the extra-islet surrounding borders ($p > 0.05$).

Six out of 18 eyes (33.3%) developed ORT at the end of the follow-up. Interestingly, ORT onset occurred independently of the progression of atrophy. The presence of a partially preserved ellipsoid zone was a mandatory condition for the development of ORT. In the case of a still present ellipsoid zone, we interpreted the ORT formation as the result of a circular and centripetal migration of the residual photoreceptors with the fusion with the attenuated ELM, with the simultaneous RPE degeneration, followed by the atrophic progression (Fig. 3). On the contrary, in the presence of a partially preserved RPE together with the absence of the ellipsoid zone beyond, we observed only a progression of the atrophy, without ORT formation (Fig. 3).

The reduction of the partially preserved retinal islet was detected in both sides of the structural OCT line (Fig. 4), with possible asymmetric course (Fig. 4).

The correlation analyses disclosed a significant negative association between retinal atrophy progression and both ELM reflectivity (Tau-Kendall coeff. -0.398 ; $p < 0.01$) and ELM thickness (Tau-Kendall coeff. -0.387 ; $p < 0.01$). Furthermore, a statistically significant correlation between atrophy progression and both CC VD in the surrounding borders (Tau-Kendall coeff. -0.42 ; $p < 0.01$), and CC VD in the region of atrophy progression (Tau-Kendall coeff. -0.51 ; $p < 0.01$) was found. CC VD values in the surrounding borders and CC VD values in the region of atrophy progression correlated also with ELM reflectivity (Tau-Kendall coeff. 0.32 ; $p < 0.01$ and 0.38 ; $p < 0.01$, respectively) and ELM thickness (Tau-Kendall coeff. 0.29 ; $p < 0.01$ and 0.34 ; $p < 0.01$, respectively).

Overall reproducibility and repeatability were 0.88 (range $0.85\text{--}0.92$; $p < 0.01$) and 0.89 (range $0.85\text{--}0.93$; $p < 0.01$), respectively. ICC was 0.88 (range $0.86\text{--}0.91$; $p < 0.01$).

DISCUSSION

The ELM originates from the fusion of the apical processes of Müller cells with the inner segments of the photoreceptor cells [7, 8]. Both Müller cells and photoreceptors have been implicated in the complex pathogenesis of CHM [6]. In the present study, we aimed to quantitatively investigate ELM in CHM, as potential biomarker of CHM clinical course and progression.

Our results showed a baseline significant thinning and reflectivity reduction in ELM of CHM patients compared to healthy controls.

ELM changes were more pronounced in those retinal regions which undergo atrophic expansion. In particular, ELM changes correlated with the atrophic progression, represented by area reduction of the partially preserved retinal islet.

A correlation was found between retinal atrophy progression and both ELM reflectivity and thickness. CC VD values in the surrounding borders correlated with ELM reflectivity and, in addition, CC VD reduction was detected in the borders evolving to atrophy.

The CHM vascular involvement is demonstrated on OCTA by the VD difference between partially preserved retinal islet and atrophic retina. Indeed, SCP and CC resulted preserved in the islet, whereas DCP appeared disrupted both in the islet and in the atrophic retina [9]. In addition, the amount and localization

of the vascular involvement significantly correlated with the impairment of the retinal structures, represented by the thinning of the retinal layers [10]. Interestingly, retinal layer impairment is not exclusively detected in the atrophic retina, since it was significantly marked also in the partially preserved retinal islet [10].

According with the current literature, potential biomarkers to analyze CHM progression include fundus autofluorescence, EZ, RPE and hyperreflective foci on OCT, microperimetry, and VD on OCTA [9–12]. The present investigation suggests that the quantitative evaluation of ELM may have a role in the estimation of the changes occurring in CHM, especially analyzing ELM thickness and reflectivity. Furthermore, ELM contributes to ORT pathogenesis, supplying the surrounding border of this outer retinal alteration.

CC in CHM may be subdivided into distinct regions on OCTA imaging. In particular, a normally appearing CC, corresponding to the partially preserved islet, is surrounded by a CC with reduced VD. This extended CC disclosed VD values similar to the CC in the region of the islet undergoing atrophy progression. Moreover, at the last follow-up, the partially preserved islet, although resulting smaller than at baseline, maintained the same configuration, with a portion of the CC extending over the borders of the partially preserved islet.

Overall, these findings further support the hypothesis of a primary degeneration both of the Müller cells and outer retina [6], followed only in a second phase by vascular perfusion impairment.

Müller cells are responsible of metabolic equilibrium maintenance within the retina [13]. ELM, intended as a biomarker directly related to the status of Müller cells and of photoreceptors, can be quantitatively assessed, representing a potentially useful indicator for the CHM diagnostic workup, with potential reference to the atrophic progression.

ORT represent a frequent finding in CHM and have been interpreted as the result of a circular rearrangement of degenerating photoreceptors [14, 15]. In the present study, we described the formation of ORT as the result of a centripetal and circular migration of the ellipsoid zone remnants, together with the fusion of the surrounding ELM and the loss of the exposed RPE cells. In this context, we found consistently the presence of partially intact ellipsoid zone and ELM; otherwise, the sole loss of RPE cells with increased atrophic change occurs.

We are aware that our study has several limitations, first of all related to the intrinsic drawbacks of OCT techniques [16]. Equally, although CHM is a rare disease, we acknowledge that the small number of patients and the inclusion of both eyes into the analyses may reduce statistical power of the study. In more detail, the limited sample may be the cause of the absence of a statistically difference in the progression of the atrophy area, although we registered smaller values of the partially preserved retinal islet area, compared to baseline. Moreover, our ELM quantitative assessment along with the hypothesis about ORT development are merely based on our interpretation of the images and would benefit from future histologic confirmations, especially to assess the timing and mechanisms of retinal remodelling and its morpho-functional deterioration. For all the above-mentioned reasons, further studies are warranted to validate the role of ELM quantitative analysis in the assessment and monitoring of CHM.

In conclusion, we described a significant involvement of ELM thickness and reflectivity in CHM. Furthermore, the deep quantitative assessment of CC allowed to detect three differentially impaired retinal regions. The ELM impairment was directly related to the progression of outer retinal atrophy and to the formation of ORT. Furthermore, the detailed categorization of different retinal regions might provide interesting perspectives in terms of future gene therapy administration planning.

SUMMARY

What was known before

- Choroideremia is characterized by outer and inner retinal changes with a partially-spared central retinal islet.
- Microstructural alterations and timing of degeneration are still partially understood.

What this study adds

- This paper specifically assessed the impairment of the external limiting membrane in Choroideremia.
- ELM changes correlated with the progression of atrophy and were also associated to three different choriocapillaris regions detectable on optical coherence tomography angiography.

REFERENCES

1. MacDonald IM, Sereda C, McTaggart K, Mah D. Choroideremia gene testing. *Expert Rev Mol Diagn.* 2004;4:478–84.
2. Karna J. Choroideremia. A clinical and genetic study of 84 Finnish patients and 126 female carriers. *Acta Ophthalmol Suppl.* 1986;176:1–68.
3. Roberts MF, Fishman GA, Roberts DK, Heckenlively JR, Weleber RG, Anderson RJ, et al. Retrospective, longitudinal, and cross sectional study of visual acuity impairment in choroideraemia. *Br J Ophthalmol.* 2002;86:658–62.
4. Chan SC, Bubela T, Dimopoulos IS, Freund PR, Varkouhi AK, MacDonald IM. Choroideremia research: Report and perspectives on the second international scientific symposium for choroideremia. *Ophthalmic Genet.* 2016;6810:1–9.
5. Zinkernagel MS, MacLaren RE. Recent advances and future prospects in choroideremia. *Clin Ophthalmol.* 2015;9:2195–200.
6. Jacobson SG, Cideciyan AV, Sumaroka A, Aleman TS, Schwartz SB, Windsor EAM, et al. Remodeling of the human retina in choroideremia: rab escort protein 1 (REP-1) mutations. *Investig Ophthalmol Vis Sci.* 2006;47:4113–20.
7. Bringmann A, Pannicke T, Grosche J, Francke M, Wiedemann P, Skatchkov S, et al. Müller cells in the healthy and diseased retina. *Prog Retin Eye Res.* 2006;25:397–424.
8. Omri S, Omri B, Savoldelli M, Jonet L, Thillaye-Goldenberg B, Thuret G, et al. The outer limiting membrane (OLM) revisited: clinical implications. *Clin Ophthalmol.* 2010;4:183–95.
9. Battaglia Parodi M, Arrigo A, MacLaren RE, Aragona E, Toto L, Mastropasqua R, et al. Vascular alterations revealed with optical coherence tomography angiography in patients with choroideremia. *Retina.* 2019;39:1200–5.
10. Arrigo A, Romano F, Parodi MB, Charbel Issa P, Birtel J, Bandello F, et al. Reduced vessel density in deep capillary plexus correlates with retinal layer thickness in choroideremia. *Br J Ophthalmol.* 2020; bjophthalmol-2020-316528.
11. Romano F, Arrigo A, MacLaren RE, Charbel Issa P, Birtel J, Bandello F, et al. Hyperreflective foci as a pathogenetic biomarker in choroideremia. *Retina.* 2020; 40:1634–40.
12. Birtel J, Salvetti AP, Jolly JK, Xue K, Gliem M, Muller PL, et al. Near-infrared autofluorescence in choroideremia: anatomic and functional correlations. *Am J Ophthalmol.* 2019;199:19–27.
13. Reichenbach A, Bringmann A. Glia of the human retina. *Glia.* 2020;68:768–96.
14. van Schuppen SM, Talib M, Bergen AA, ten Brink JB, Florijn RJ, Boon CJF, et al. Long-term follow-up of patients with choroideremia with scleral pits and tunnels as a novel observation. *Retina.* 2018;38:1713–24.
15. Zweifel SA. Outer retinal tubulation: a novel optical coherence tomography finding. *Arch Ophthalmol.* 2009;127:1596–602.
16. Spaide RF, Fujimoto JG, Waheed NK, Sadda SR, Staurenghi G. Optical coherence tomography angiography. *Prog Retin Eye Res.* 2018;64:1–55.

AUTHOR CONTRIBUTIONS

AA, MBP: study design, data analysis, data interpretation, manuscript drafting. EA, AP, FC: data collection, data analysis, manuscript revision. FB, REM: study supervision, data interpretation, manuscript revision.

COMPETING INTERESTS

FB consultant for Alcon (Fort Worth, TX, USA), Alimera Sciences (Alpharetta, GA, USA), Allergan Inc (Irvine, CA, USA), Farmila-Thea (Clermont-Ferrand, France), Bayer Shering-

Pharma (Berlin, Germany), Bausch And Lomb (Rochester, NY, USA), Genentech (San Francisco, CA, USA), Hoffmann-La-Roche (Basel, Switzerland), NovagaliPharma (Évry, France), Novartis (Basel, Switzerland), Sanofi-Aventis (Paris, France), Thrombogenics (Heverlee, Belgium), Zeiss (Dublin, USA). RM is a consultant to Biogen (Boston, USA). All other authors have no disclosures to declare.

ADDITIONAL INFORMATION

Supplementary information The online version contains supplementary material available at <https://doi.org/10.1038/s41433-022-01953-3>.

Correspondence and requests for materials should be addressed to Alessandro Arrigo.

Reprints and permission information is available at <http://www.nature.com/reprints>

Publisher's note Springer Nature remains neutral with regard to jurisdictional claims in published maps and institutional affiliations.